

Corrosion Behavior of a Superduplex Stainless Steel in Chloride Aqueous Solution

Manuele Dabalà, Irene Calliari, and Alessandra Variola

(Submitted 12 September 2002; in revised form 6 January 2004)

Super duplex stainless steels (SDSS) have been widely used as structural materials for chemical plants (especially in those engaged in phosphoric acid production), in the hydrometallurgy industries, and as materials for offshore applications due to their excellent corrosion resistance in chloride environments, compared with other commercial types of ferritic stainless steels. These alloys also possess superior weldability and better mechanical properties than austenitic stainless steels. However, due to their two-phase structure, the nature of which is very dependent on their composition and thermal history, the behavior of SDSS regarding localized corrosion appears difficult to predict, especially in chloride environments. To improve their final properties, the effect of the partition of the alloying elements between the two phases, and the composition and microstructure of each phase are the key to understanding the localized corrosion phenomena of SDSS. This paper concerns the effects of the SDSS microstructure and heat treatment on the SDSS corrosion resistance in aqueous solutions, containing different amounts of NaCl at room temperature.

Keywords: chlorides, corrosion resistance, heat treatments, pitting, secondary austenite, super duplex stainless steels

1. Introduction

Super duplex stainless steels (SDSS) may be defined as a group of steels having a two phase ferrite-austenite microstructure after heat treatment and water quenching, with a pitting resistance equivalent number (PREN) higher than 40. The PREN value is linked to the content of the three most important elements in the alloy, namely, Cr, Mo, and N, with each of them weighted according to its influence on pitting.^[1] The approximately equal volume fractions of ferrite and austenite are achieved by the simultaneous control of the chemical composition and the annealing temperature. These alloys have been widely used as structural materials for chemical plants, especially those engaged in phosphoric acid production, in the hydrometallurgy industries, and as materials for offshore applications due to their excellent corrosion resistance in chloride environments, compared with other commercial types of ferritic stainless steels. These alloys also possess superior weldability and better mechanical properties than austenitic stainless steels. However, due to their two-phase structure, the nature of which is very dependent on their composition and thermal history, the behavior of SDSS regarding localized corrosion appears difficult to predict. To improve their final properties,

the effect of the partition of the alloying elements between the two phases, and the composition and microstructure of each phase are the key to understanding the localized corrosion phenomena of SDSS. Chloride solutions are the most widespread environments responsible for localized corrosion of SDSS, and the aggressiveness of the environment increases with chloride content, redox potential, activity, and temperature. This article reports on the effect of the composition and microstructure of the alloy, and heat treatment on the corrosion resistance of an EN 1.4501 SDSS in aqueous solutions containing different amounts of NaCl at room temperature.

2. Experimental

The composition and PREN value of the EN 1.4501 SDSS are reported in Table 1. The steel (10 mm diameter) was subjected to hot working at various temperatures (1050, 1150, 1250, 1300, and 1350 °C) in an inert atmosphere and was cooled in air before immersion in a chloride solution for the corrosion tests. The mean area reduction was about 83%. Samples of steels that were 10 mm diameter were obtained from the hot-worked material.^[2]

Metallurgical characterization was performed by means of optical microscopy (OM) and scanning electron microscopy (SEM). The ferrite content was measured by means of image analysis, taking 10 measurements at a magnification of $\times 100$ on samples etched with Beraha's reagent. The Vickers microhardness was measured (Werlag microhardness tester, Leitz, Berlin, Germany) using a 100 g load. The chemical compositions of ferrite and austenite were determined by means of energy dispersive spectrometry (EDS) with the quantitative analysis performed using a standardless ZAF [ZAF = atomic number (z), absorption, fluorescence] correction.

Manuele Dabalà, Irene Calliari, and Alessandra Variola, Department of Mechanical and Management Innovation (DIMEG), Università di Padova, Via Marzolo 9, 35131 Padova, Italy. Contact e-mail: manuele.dabala@unipd.it.

Table 1 Chemical Composition (wt.%) and PREN Value of the Examined Material

C	Si	Mn	Cr	Ni	Mo	Cu	W	P	S	N	PREN
0.030	0.26	0.40	25.08	7.29	3.43	0.55	0.53	0.023	0.001	0.272	42

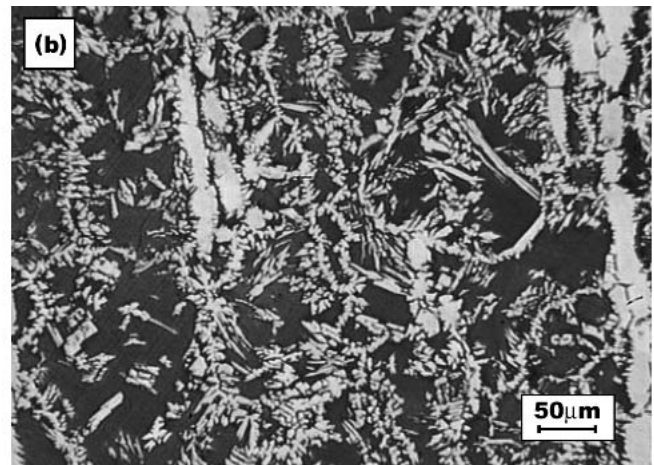
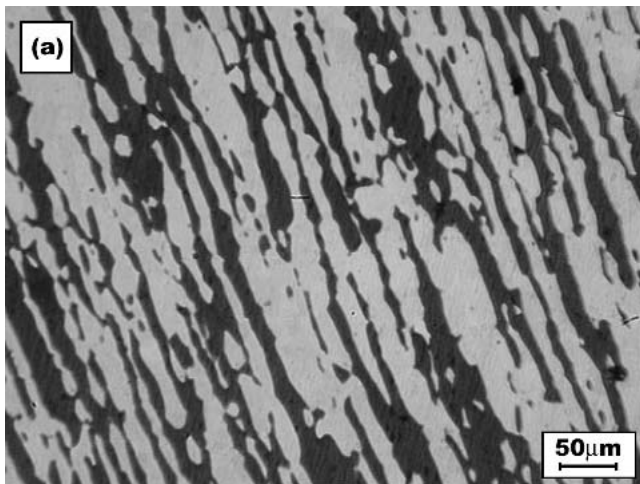


Fig. 1 Microstructure of the steel after heat treatment at 1050 °C (a) and at 1350 °C (b)

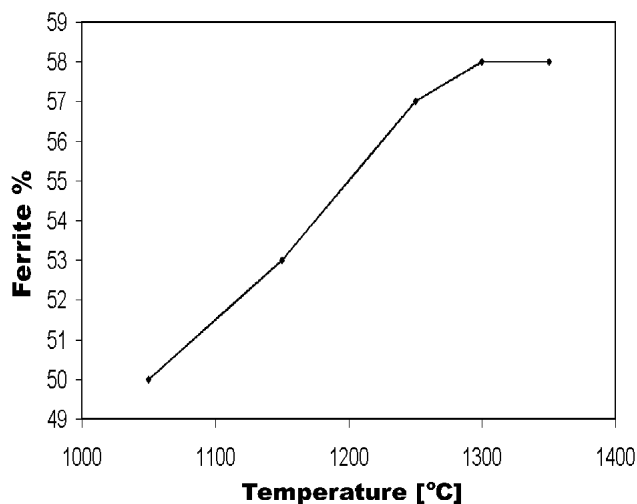


Fig. 2 Percentage of ferrite vs temperature

Table 2 Alloying Elements Content in Ferrite and Austenite (a)

Temperature, °C	Cr		Mo		Ni		W	
	A	F	A	F	A	F	A	F
1050	24.8	27.6	2.9	6.6	8.3	5.5	0.7	0.9
1150	24.8	27.2	3.2	6.6	8.5	5.6	0.8	1.2
1250	24.8	26.7	3.0	6.0	8.6	6.3	0.6	1.2
1300	25.1	26.2	3.0	6.2	8.7	6.6	0.7	1.0
1350	25.4	26.6	3.1	5.4	8.6	6.8	0.8	0.8

(a) A, austenite; F, ferrite.

The corrosion tests were performed in 0.1 M H₂SO₄ aqueous solutions with different concentrations of NaCl (0-0.5 M, 1.5 M, 2.5 M, and 3.5 M). The polarization curves were performed by means of a potentiostat AMEL 551 (Milano, Italy) equipped with function generator. The scan rate was 0.5 mV/s.

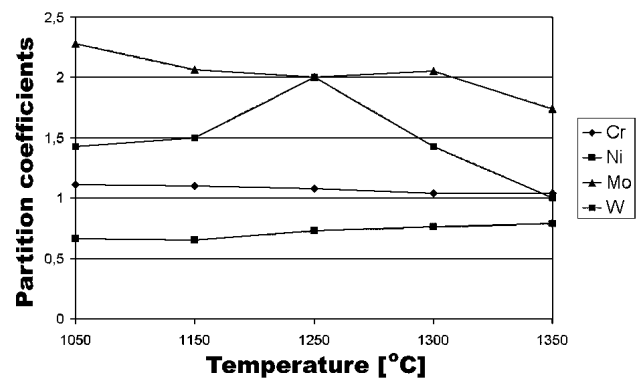


Fig. 3 Partition coefficient of the elements

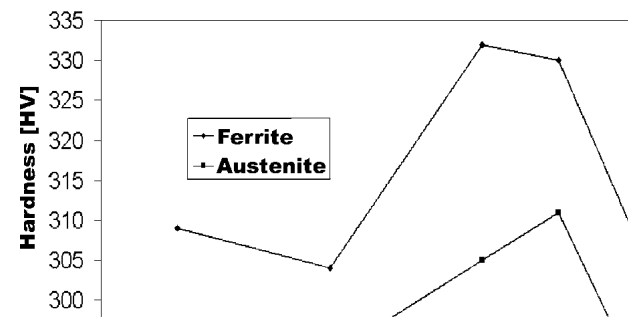


Fig. 4 Vickers hardness of the two phases of the steel

3. Results and Discussion

From the OM analysis (Fig. 1) of the annealed samples, it is very evident that the dual-phase ferrite-austenite structure has evolved. It is also clear that an increase of ferrite has occurred with the increase in the annealing temperature, as shown in Fig. 2.

As is well known, ferrite content increases with temperature, and the value is closely related to the chemical composition, which may be roughly expressed as the Cr/Ni ratio.^[3] The

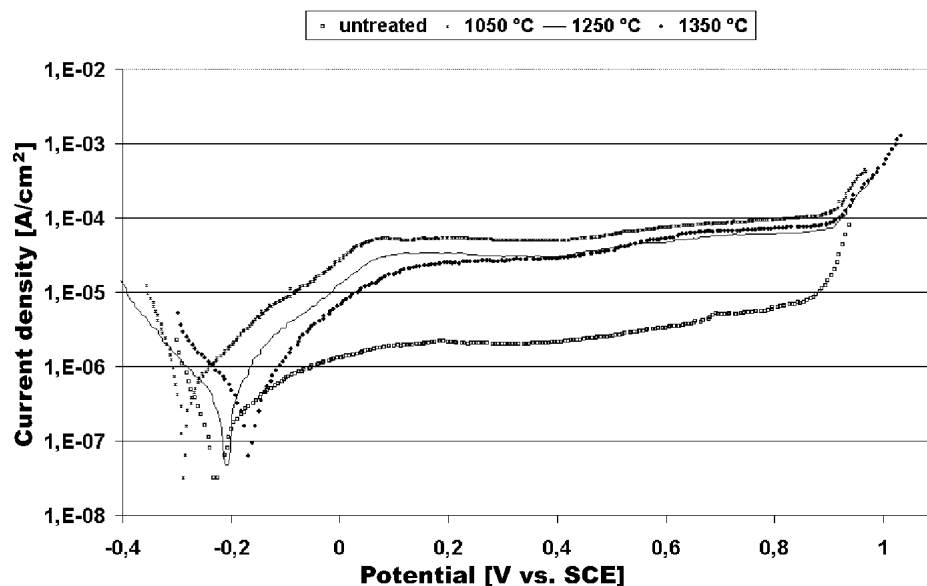


Fig. 5 Potentiodynamic curves in a solution of H₂SO₄ 0.1 M, NaCl 2.5 wt.% solution.

Table 3 Free Corrosion Current and Passive Current in Different Electrolytes for Different Heat Treatments

Temperature, °C		0.1 M H ₂ SO ₄	0.1 M H ₂ SO ₄ + 0.5% NaCl	0.1 M H ₂ SO ₄ + 1.5% NaCl	0.1 M H ₂ SO ₄ + 2.5% NaCl	0.1 M H ₂ SO ₄ + 3.5% NaCl
1050	<i>i</i> _{corr}	6.15 E-6	2.20 E-6	8.37 E-7	1.00 E-6	3.87 E-7
	<i>i</i> _p	3.65 E-5	3.05 E-5	6.18 E-5	5.99 E-5	4.44 E-5
1150	<i>i</i> _{corr}	1.82 E-7	1.46 E-7	1.82 E-7	2.18 E-7	1.46 E-7
	<i>i</i> _p	6.19 E-7	1.49 E-6	2.70 E-6	6.63 E-6	1.12 E-5
1250	<i>i</i> _{corr}	3.56 E-7	4.20 E-7	2.26 E-7	2.69 E-7	1.93 E-7
	<i>i</i> _p	6.16 E-7	4.49 E-6	1.20 E-5	1.69 E-5	2.65 E-5
1300	<i>i</i> _{corr}	4.42 E-7	2.81 E-7	2.00 E-7	3.20 E-7	1.61 E-7
	<i>i</i> _p	9.62 E-7	5.33 E-6	2.97 E-6	3.57 E-5	5.45 E-5
1350	<i>i</i> _{corr}	7.63 E-7	1.53 E-6	2.48 E-6	4.76 E-7	3.5 E-7
	<i>i</i> _p	1.91 E-6	1.75 E-5	3.04 E-5	4.41 E-5	6.04 E-5

Free corrosion current (*i*_{corr}), passive current (*i*_p).

microstructure of the sample treated at 1350 °C appears to be quite different from that of the others. The precipitation of a secondary austenite phase (γ_2) was observed. The formation of γ_2 occurs particularly when the alloy undergoes heat treatment at high solution annealing temperatures coupled with a slow cooling rate.^[4] Other secondary phases have not been seen during the SEM-EDS investigation. Cr, Mo, Ni and W contents in the ferrite and austenite were determined by means of EDS and are reported in Table 2. The ratios among Cr, Ni, and Mo in ferrite and austenite (i.e., the partition coefficient) are reported in Fig. 3.

The ferrite is rich in α -stabilizing elements (in order of effectiveness: Mo > W > Cr), and the austenite is rich in γ -stabilizing elements (in order of effectiveness: Ni > Mn). As the temperature increases, a weak depletion of Cr and Mo and a weak enrichment of Ni in ferrite are recorded. Moreover, the partition coefficients of the elements vary very little with temperature. This is probably due to the fact that, for the concentrations and temperatures concerned, the solubility limits for these elements have not been exceeded.

The microhardness values of ferrite and austenite are reported in Fig. 4. It is worth noting that the ferrite hardness is higher than the austenite hardness^[5] and that the hardness of the ferrite increases with increasing temperature. This is in agreement with the variation in chemical composition. In fact, the small increase of Ni in ferrite with temperature causes an increase in the strength of the solid solution.

The corrosion measurements are shown in Fig. 5. All of the samples show similar corrosion resistance, with the passive region appearing to be unaffected by the annealing temperature. This is in agreement with the weak variation in both chemical composition and hardness. However, as reported in Table 3, the free corrosion current and the passive current show a weak minimum for samples annealed at about 1250 °C in all NaCl environments. From an analysis of the corroded samples, selective corrosion of the ferrite grains was detected in the samples treated at temperatures below 1300 °C. This is probably due to the weak increase in the amount of Ni in the ferrite with the temperature. The incorporation of Ni in ferrite, besides providing strength to the ferrite solid solution, also increases its

corrosion resistance. Because the corrosion resistance is determined by the phase with the lowest susceptibility to chemical attack, such as in ferrite,^[6] the increase in corrosion resistance of this phase improves the overall corrosion resistance of the alloy. The samples that were heat treated at 1300 °C, and especially for those heat treated at 1350 °C, showed selective corrosion of the secondary austenite (γ_2) grains. The γ_2 precipitates are poorer in N, Cr, and Mo than is the primary austenite that is formed at higher temperatures and, thus, results in low corrosion resistance.^[7] Because a lower corrosion resistance is recorded for the samples treated at 1300 °C, and especially at 1350 °C, it is evident that the γ_2 precipitates are the phase with the lowest ability to resist the chloride solution and are, thus, mainly responsible for the corrosion of these alloys.

4. Conclusions

The microstructure, the chemical composition of the phases, and the corrosion resistance of the alloys are weakly affected by the annealing heat treatment temperature. In fact, little variation in ferrite content and partition coefficient was observed. However, the corrosion resistance showed a slight increase at temperatures lower than 1300 °C due to the improvement in the corrosion resistance of the ferrite, which is the main phase responsible for the overall corrosion behavior of the alloy. The ferrite grows rich in Ni with the temperature, thereby increasing its corrosion resistance. However, at temperatures

higher than 1300 °C, γ_2 precipitation occurs, and because this phase is poorer in N, Cr, and Mo than is the primary austenite formed at higher temperatures, a decrease in the corrosion resistance is observed.

References

1. P. Combrade and J.P. Audouard: "Duplex Stainless Steel and Localized Corrosion Resistance" in *Proc. Duplex Stainless Steels Conference*, J. Charles and S. Bernhardsson, ed., Les Éditions de Physique, Les Ulis, France, 1991, pp. 257-81.
2. E. Ramous, I. Calliari, E. Nocerino, and P. Gasparella: "High Temperature Influence on Microstructure of Duplex Stainless Steel" in *Proc. 6th World Duplex Conference*, Venice, Italy, Associazione Italiana di Metallurgia, Italy, 17-20 Oct 2000, pp. 425-30.
3. X.G. Wang, D. Dumortier, and Y. Riquier: "Structural Evolution of Zeron 100 Duplex Stainless Steel Between 550 and 1100 °C" in *Proc. Duplex Stainless Steels Conference*, Beaune, France, J. Charles and S. Bernhardsson, ed., Les Éditions de Physique, Les Ulis, France, 1991, pp. 127-34.
4. J. Charles: "Why and Where Duplex Stainless Steels" in *Proc. 5th World Duplex Stainless Steels Conference*, KCI Publishing BV, Maasticht, Netherlands, 1997, pp. 29-42.
5. U. Draugelates, A. Schram, and C. Boppert: "Effect of the Thermal Welding Process Conditions on the Structure and Properties in the HAZ of Duplex Cast Steel" in *Proc. Duplex Stainless Steels Conference*, Beaune, France, J. Charles and S. Bernhardsson, ed., Les Éditions de Physique, Les Ulis, France, 1991, pp. 985-92.
6. V. Cihal: *Intergranular Corrosion of Steels and Alloys*, Elsevier Science, Amsterdam, Netherlands, 1984, p. 31.
7. H.S. Wang, L.J. Power, S. Cardno, C.D. Stewart, and G. Warburton: *Stainless Steels World*, KCI Publishing BV, The Hague, Netherlands, 1999, pp. 507-18.